

Is the relativistic distorted-wave impulse approximation useful to nuclear reaction?*

K. Miyazaki

Abstract

We have reconsidered the nonrelativistic distorted-wave t -matrix approximation (NR-DWTA) for proton knockout ($p, 2p$) reaction using modern high-quality phenomenological optical potentials and NN t -matrix. We have calculated $^{40}\text{Ca}(p, 2p)$ reactions at $T_{LAB} = 200$ MeV and compared the results with the relativistic distorted-wave impulse approximation (RDWIA) calculations. It is found that the NR-DWTA is superior to the RDWIA in consistent description of the cross section and the analyzing power. An immediate relativistic extension of the DWIA to the nuclear reaction has a problem.

1 Introduction

It seems that the success of the relativistic impulse model for proton-nucleus (p-A) elastic scattering [1,2] inspires us to apply it to other p-A scatterings and reactions. Recent high-quality phenomenological relativistic optical model potentials [3,4] and nucleon-nucleon (NN) t -matrix [5] have made such attempts possible. One of the most thoroughgoing investigations among them is the RDWIA description of the ($p, 2p$) reaction by Cooper and Maxwell [6]. The result of their enormous numerical calculations is however somewhat discouraging. It is not obviously superior to the old calculation [7] based on the NR-DWTA, which used the nonrelativistic nonglobal optical potentials by interpolating them and the nonrelativistic Love-Franey NN t -matrix. It is therefore worthwhile to perform the NR-DWTA calculation using new relativistic inputs of the optical potential and the NN t -matrix. Such a calculation becomes an extensive test of them. Furthermore the comparison of it with the result of Ref. [6] provides us an insight on the validity of the relativistic approach to nuclear reactions.

In the next section we review the NR-DWTA formalism for ($p, 2p$) reaction. The relevant factorized NN t -matrix is evaluated explicitly in section 3. The numerical results are shown and discussed in comparison with RDWIA results in section 4. Finally, our conclusion is drawn in section 5.

*This paper is the revised version of CDS ext-2003-007. Some texts and mistypes have been corrected.

2 The formalism of NR-DWTA

Although there are several review articles [8-12] and textbooks [13,14] for $(p, 2p)$ reaction, we here review the NR-DWTA briefly for the discussion in §4. The t -matrix for $(p, 2p)$ reaction in the nonrelativistic distorted-wave impulse approximation (NR-DWIA) is

$$T_{(p,2p)} = \left\langle \psi_1^{(-)} \psi_2^{(-)} \left| t_{pp} \right| \psi_0^{(+)} \phi_t \right\rangle, \quad (1)$$

where $\psi_0^{(+)}$ and $\psi_{1(2)}^{(-)}$ are the distorted waves of the incoming (0) and two outgoing (1 and 2) protons, ϕ_t is a single-particle bound-state wave function of the knocked-out proton (t) in the target nucleus (or more precisely speaking, an overlap function between the wave functions of target and residual nucleus) and t_{pp} is the t -matrix operator for proton-proton (p-p) scattering in free space. For simplicity, the spin-orbit distortions are neglected.

Equation (1) is represented in momentum space as

$$T_{(p,2p)} = \left\langle \psi_1^{(-)} \left| \mathbf{p}_1 \right\rangle \left\langle \psi_2^{(-)} \left| \mathbf{p}_2 \right\rangle \left\langle \mathbf{p}_1 \mathbf{p}_2 \left| t_{pp} \right| \mathbf{p}_0 \mathbf{p}_t \right\rangle \left\langle \mathbf{p}_0 \left| \psi_0^{(+)} \right\rangle \left\langle \mathbf{p}_t \left| \phi_t \right\rangle. \quad (2)$$

Introducing the reduced p-p t -matrix

$$\left\langle \mathbf{p}_1 \mathbf{p}_2 \left| t_{pp} \right| \mathbf{p}_0 \mathbf{p}_t \right\rangle = \delta^3(\mathbf{p}_1 + \mathbf{p}_2 - \mathbf{p}_0 - \mathbf{p}_t) \left\langle \mathbf{p}_1 \mathbf{p}_2 \parallel t_{pp} \parallel \mathbf{p}_0 \mathbf{p}_t \right\rangle, \quad (3)$$

we then factorize it as

$$\left\langle \mathbf{p}_1 \mathbf{p}_2 \parallel t_{pp} \parallel \mathbf{p}_0 \mathbf{p}_t \right\rangle \rightarrow \left\langle \mathbf{k}_1 \mathbf{k}_2 \parallel t_{pp} \parallel \mathbf{k}_0 \mathbf{k}_t \right\rangle, \quad (4)$$

where \mathbf{k}_0 , \mathbf{k}_1 and \mathbf{k}_2 are the asymptotic momenta of the incoming and two outgoing protons in the p-A c.m. frame and \mathbf{k}_t is restricted by the momentum conservation:

$$\mathbf{k}_t = \mathbf{k}_1 + \mathbf{k}_2 - \mathbf{k}_0. \quad (5)$$

As a result,

$$T_{(p,2p)} = \left\langle \mathbf{k}_1 \mathbf{k}_2 \parallel t_{pp} \parallel \mathbf{k}_0 \mathbf{k}_t \right\rangle \left[\left\langle \psi_1^{(-)} \left| \mathbf{p}_1 \right\rangle \left\langle \psi_2^{(-)} \left| \mathbf{p}_2 \right\rangle \left\langle \mathbf{p}_0 \left| \psi_0^{(+)} \right\rangle \left\langle \mathbf{p}_1 + \mathbf{p}_2 - \mathbf{p}_0 \left| \phi_t \right\rangle \right] . \quad (6)$$

This is an essential expression of the NR-DWTA for $(p, 2p)$ reaction.

The actual calculation is performed in coordinate space:

$$\begin{aligned} T_{(p,2p)} &= \left\langle \mathbf{k}_1 \mathbf{k}_2 \parallel t_{pp} \parallel \mathbf{k}_0 \mathbf{k}_t \right\rangle \left[\left\langle \psi_1^{(-)} \left| \mathbf{r}_1 \right\rangle \left\langle \mathbf{r}_1 \left| \mathbf{p}_1 \right\rangle \left\langle \psi_2^{(-)} \left| \mathbf{r}_2 \right\rangle \left\langle \mathbf{r}_2 \left| \mathbf{p}_2 \right\rangle \right. \right. \\ &\quad \left. \left. \times \left\langle \mathbf{p}_0 \left| \mathbf{r}_0 \right\rangle \left\langle \mathbf{r}_0 \left| \psi_0^{(+)} \right\rangle \left\langle \mathbf{p}_1 + \mathbf{p}_2 - \mathbf{p}_0 \left| \mathbf{r}_t \right\rangle \left\langle \mathbf{r}_t \left| \phi_t \right\rangle \right] . \quad (7) \end{aligned}$$

Using

$$\left\langle \mathbf{p}_1 + \mathbf{p}_2 - \mathbf{p}_0 \left| \mathbf{r}_t \right\rangle = \left\langle \mathbf{p}_1 \left| \mathbf{r}_t \right\rangle \left\langle \mathbf{p}_2 \left| \mathbf{r}_t \right\rangle \left\langle \mathbf{r}_t \left| \mathbf{p}_0 \right\rangle, \quad (8)$$

We finally obtain

$$T_{(p,2p)} = \langle \mathbf{k}_1 \mathbf{k}_2 \| t_{pp} \| \mathbf{k}_0 \mathbf{k}_t \rangle \times \left[\langle \psi_1^{(-)} | \mathbf{r}_1 \rangle \langle \mathbf{r}_1 | \mathbf{r}_t \rangle \langle \psi_2^{(-)} | \mathbf{r}_2 \rangle \langle \mathbf{r}_2 | \mathbf{r}_t \rangle \langle \mathbf{r}_t | \mathbf{r}_0 \rangle \langle \mathbf{r}_0 | \psi_0^{(+)} \rangle \langle \mathbf{r}_t | \phi_t \rangle \right], \quad (9)$$

$$= \langle \mathbf{k}_1 \mathbf{k}_2 \| t_{pp} \| \mathbf{k}_0 \mathbf{k}_t \rangle \int d^3 \mathbf{r} \psi_1^{(-)*}(\mathbf{r}) \psi_2^{(-)*}(\mathbf{r}) \psi_0^{(+)}(\mathbf{r}) \phi_t(\mathbf{r}). \quad (10)$$

The integral of Eq. (10) is called as the distorted momentum distribution. Usually, the argument \mathbf{r} in the initial distorted-wave function is multiplied by a factor $1 - 1/A$ [14], where A is the mass number of the target nucleus. In this work, such a factor is ignored because other $1/A$ effects, the coupling term between the coordinates of two outgoing protons [14] and the recoil term [9], have already been neglected from the first.

The DWTA is often referred as a zero-range approximation. This term is however misleading. In the model of NN t -matrix using one-boson exchange potentials, the zero-range means infinite masses of the mesons. Such a situation is unphysical while the DWTA is a reasonable physical prescription as will be discussed in section 4.

3 The factorized NN t -matrix

Here we show explicit expression of the factorized NN t -matrix in Eq. (4). The relativistic model of Ref. [5] enables us to calculate it directly:

$$\langle \mathbf{k}_{1A} \mathbf{k}_{2A} \| t_{pp} \| \mathbf{k}_{0A} \mathbf{k}_{tA} \rangle = \bar{u}_1(\mathbf{k}_{1A}) \bar{u}_2(\mathbf{k}_{2A}) \hat{t}_{pp}^{as} u_1(\mathbf{k}_{0A}) u_2(\mathbf{k}_{tA}), \quad (11)$$

where the Dirac spinor $u_{1(2)}(\mathbf{k}_{iA})$ ($i = 0, 1, 2$ and t) is

$$u_{1(2)}(\mathbf{k}_{iA}) = N_{iA} \begin{pmatrix} 1 \\ \boldsymbol{\sigma}_{1(2)} \cdot \mathbf{k}_{iA} / (E_{iA} + M) \end{pmatrix}, \quad (12)$$

and

$$N_{iA} = \left(\frac{E_{iA} + M_p}{2E_{iA}} \right)^{1/2}. \quad (13)$$

M_p is the mass of a proton, E_{iA} ($i = 0, 1$ and 2) are the total energies of the incoming and two outgoing protons and $E_{tA} = E_{1A} + E_{2A} - E_{0A}$. In this section, the momentums in the p-A c.m. and laboratory frame are attached by subscripts A and L respectively. It is well known that the target proton (t) in nucleus is off the mass shell, $E_{tA}^2 - \mathbf{k}_{tA}^2 \neq M_p^2$. However, we use free proton mass because the phenomenological NN t -matrix is valid only for it. Anti-symmetric p-p t -matrix operator \hat{t}_{pp}^{as} in Eq. (11) is given by

$$\hat{t}_{pp}^{as} = \sum_{i=S,V,T,A,P} f_i^{as} \hat{\lambda}_{1i} \hat{\lambda}_{2i}, \quad (14)$$

$$f_i^{as} = f_i(q^2) - \sum_{j=S,V,T,A,P} \alpha_{ji} f_j(Q^2), \quad (15)$$

where $\hat{\lambda}_i$ are the complete sets of 4×4 matrix, α_{ji} is the Fierz matrix, f_i is the invariant Fermi amplitude, and $q^\mu = (E_{1A} - E_{0A}, \mathbf{k}_{1A} - \mathbf{k}_{0A})$ and $Q^\mu = (E_{2A} - E_{0A}, \mathbf{k}_{2A} - \mathbf{k}_{0A})$ are the direct and exchange four-momentum transfers.

Equation (11) is expanded in Pauli spinor space as

$$\begin{aligned} & \bar{u}_1(\mathbf{k}_{1A}) \bar{u}_2(\mathbf{k}_{2A}) \hat{t}_{pp}^{as} u_1(\mathbf{k}_{0A}) u_2(\mathbf{k}_{tA}) \\ &= M_{00} + iM_{y0} \sigma_{1y} + iM_{0y} \sigma_{2y} + M_{xx} \sigma_{1x} \sigma_{2x} \\ &+ M_{yy} \sigma_{1y} \sigma_{2y} + M_{zz} \sigma_{1z} \sigma_{2z} + M_{xz} \sigma_{1x} \sigma_{2z} + M_{zx} \sigma_{1z} \sigma_{2x}. \end{aligned} \quad (16)$$

In this work we suppose coplanar experiment. The incident direction is taken as z-axis and y-axis is perpendicular to the scattering plane. It is noted that the factorized NN t -matrix is evaluated in the p-A c.m. frame not in the p-p c.m. one. Thus, there are 8 Wolfenstein amplitudes $M_{\mu\nu}$ in Eq. (16). They are given by

$$M_{\mu\nu} = f_S^{as} W_S^{\mu\nu} + f_V^{as} (W_{V0}^{\mu\nu} - W_{V3}^{\mu\nu}) + 2f_T^{as} (W_{T0}^{\mu\nu} + W_{T3}^{\mu\nu}) - f_A^{as} W_{A3}^{\mu\nu}, \quad (17)$$

for $(\mu\nu) = (00), (y0), (0y)$ and (yy) , while for $(\mu\nu) = (xx), (zz), (xz)$ and (zx) ,

$$M_{\mu\nu} = -f_V^{as} W_{V3}^{\mu\nu} + 2f_T^{as} (W_{T0}^{\mu\nu} + W_{T3}^{\mu\nu}) + f_A^{as} (W_{A0}^{\mu\nu} - W_{A3}^{\mu\nu}) + f_P^{as} W_P^{\mu\nu}. \quad (18)$$

The coefficients $W_S^{\mu\nu}$ for the scalar amplitudes in Eq. (17) are

$$W_S^{00} = N (1 - X_1^0 X_1^1) (1 - X_2^t X_1^2 + X_1^t X_2^2), \quad (19)$$

$$W_S^{y0} = N X_1^0 X_2^1 (1 - X_2^t X_1^2 + X_1^t X_2^2), \quad (20)$$

$$W_S^{0y} = -N (1 - X_1^0 X_1^1) (X_1^t X_1^2 + X_2^t X_2^2), \quad (21)$$

$$W_S^{yy} = N X_1^0 X_2^1 (X_1^t X_1^2 + X_2^t X_2^2), \quad (22)$$

with

$$N = N_{0A} N_{1A} N_{2A} N_{tA}. \quad (23)$$

The quantities X_i^j are given by

$$X_1^0 = c_{0A} \frac{|\mathbf{k}_{0L}|}{E_{0A} + M_p}, \quad (24)$$

$$X_1^1 = \frac{c_{1A} |\mathbf{k}_{0L}| + \cos \theta_{1L} |\mathbf{k}_{1L}|}{E_{1A} + M_p}, \quad (25)$$

$$X_1^2 = \frac{c_{2A} |\mathbf{k}_{0L}| + \cos \theta_{2L} |\mathbf{k}_{2L}|}{E_{2A} + M_p}, \quad (26)$$

$$X_1^t = \frac{\sin \theta_{1L} |\mathbf{k}_{1L}| - \sin \theta_{2L} |\mathbf{k}_{2L}|}{E_{tA} + M_p}, \quad (27)$$

$$X_2^1 = \frac{\sin \theta_{1L} |\mathbf{k}_{1L}|}{E_{1A} + M_p}, \quad (28)$$

$$X_2^2 = \frac{\sin \theta_{2L} |\mathbf{k}_{2L}|}{E_{2A} + M_p}, \quad (29)$$

$$X_2^t = \frac{c_{tA} |\mathbf{k}_{0L}| + \cos \theta_{1L} |\mathbf{k}_{1L}| + \cos \theta_{2L} |\mathbf{k}_{2L}|}{E_{tA} + M_p}, \quad (30)$$

where \mathbf{k}_{iL} are the momentums of the incoming and two outgoing protons in the laboratory frame, the two scattering angles $\theta_{1L} (> 0)$ and $\theta_{2L} (> 0)$ are on opposite sides of the incident direction. The quantities c_{iA} ($i = 0, 1$ and 2) are defined in the Lorentz transformation of the momentums from the laboratory to p-A c.m. frame:

$$\mathbf{k}_{0A} = c_{0A} \mathbf{k}_{0L}, \quad (31)$$

$$c_{0A} = \frac{\gamma_{pA} M_A}{E_{0L} + M_A}, \quad (32)$$

$$\mathbf{k}_{1A} = \mathbf{k}_{1L} + c_{1A} \mathbf{k}_{0L}, \quad (33)$$

$$c_{1A} = \frac{1}{E_{0L} + M_A} \left(\frac{\gamma_{pA} - 1}{\mathbf{v}_{pA}^2} \mathbf{k}_{1L} \cdot \mathbf{v}_{pA} - \gamma_{pA} E_{1L} \right), \quad (34)$$

$$\mathbf{k}_{2A} = \mathbf{k}_{2L} + c_{2A} \mathbf{k}_{0L}, \quad (35)$$

$$c_{2A} = \frac{1}{E_{0L} + M_A} \left(\frac{\gamma_{pA} - 1}{\mathbf{v}_{pA}^2} \mathbf{k}_{2L} \cdot \mathbf{v}_{pA} - \gamma_{pA} E_{2L} \right), \quad (36)$$

and

$$c_{tA} = c_{1A} + c_{2A} - c_{0A}, \quad (37)$$

where M_A is the mass of the target nucleus, $\mathbf{v}_{pA} = \mathbf{k}_{0L} / (E_{0L} + M_A)$ is the velocity of the p-A c.m. in the laboratory frame and $\gamma_{pA} = (1 - \mathbf{v}_{pA}^2)^{-1/2}$. The detailed expressions of the other coefficients $W^{\mu\nu}$ in Eqs. (17) and (18) are presented in Appendix.

We have derived the factorized NN t -matrix relevant to the NR-DWTA of $(p, 2p)$ reaction by calculating it directly in terms of the Dirac spinor and the invariant Fermi amplitudes. This is an essential difference of the present calculation from old ones [7,12,16]. If we start at Wolfenstein NN amplitude in Pauli spin space as Eq. (16), we have to rotate the quantization axis in p-p c.m. frame into that in p-A c.m. frame and perform Wigner rotation further. The old NR-DWTA calculations did not take into account Wigner rotation and so are not accurate. Our method in this section can avoid such complicated procedure.

4 Numerical analyses

Although the spin-orbit distortions have been ignored for simplicity in section 2, they are necessary to calculate polarization observables. The detailed expression of the NR-DWTA t -matrix for $(p, 2p)$ reaction with spin-orbit distortions can be found in Ref. [15]. The method of 3-dimensional integration is also according to Ref. [15], in which the distorted-wave functions of two out-going protons are rotated to avoid enormous summations over the z-components of angular momentums in their partial wave expansions. This clever method saves CPU time considerably so that we are able to perform the calculations by personal computer in terms of C language.

Figures 1-4 display the energy sharing distributions of cross sections and analyzing powers for proton knockout from $1d_{3/2}$ and $1d_{5/2}$ state of ^{40}Ca at $T_{LAB} = 200$ MeV for outgoing proton angles $(\theta_{1L}, \theta_{2L}) = (29^\circ, 47^\circ)$ and $(54^\circ, 54^\circ)$. Experimental data are from Ref. [16]. The present calculations are limited to a ^{40}Ca target because the several $1/A$ effects are ignored as mentioned in section 2. The distorted waves are calculated using the optical potential GOP1 of Ref. [3]. The bound-state wave functions are calculated by the same way as Ref. [7]. The spectroscopic factor is a simple shell-model value $2j + 1$ except for normalization to the data by 0.77 for $1d_{3/2}$ at $(54^\circ, 54^\circ)$. Our results are compared with Figs. 1 and 2 in Ref. [6]. It is noted that our cross section is half of that in Ref. [6],

$$\frac{d^5\sigma}{d\Omega_{1L}d\Omega_{2L}d(E_{1L} - E_{2L})} = \frac{1}{2} \frac{d^5\sigma}{d\Omega_{1L}d\Omega_{2L}dE_{1L}}. \quad (38)$$

Typical features of our NR-DWTA results are apparent in Fig. 1. The experimental data of cross section and analyzing power are well reproduced below $E_{1L} - E_{2L} = 50$ MeV while above 50 MeV the calculated cross section is smaller and the analyzing power is much larger than the data. The RDWIA results are quite different. Its cross section shows much narrower distribution than the experimental data and our result. Its analyzing power shows a dip around $E_{1L} - E_{2L} = -60$ MeV that is absent both in the data and ours. However the data of analyzing powers above 50 MeV are well reproduced. In Fig. 2 the NR-DWTA calculation reproduces the cross section relatively well, but there still

remain small discrepancies with the data over the range of $E_{1L} - E_{2L}$. The discrepancies however become much larger in the analyzing power. To the contrary, the calculated cross section by the RDWIA has narrow distribution again, while the data of analyzing power in $E_{1L} - E_{2L} > 0$ are fairly well reproduced.

The same features as Figs. 1 and 2 are also seen in $(54^\circ, 54^\circ)$ scattering. In Fig. 3, both the cross section and analyzing power are well reproduced in all the range of $E_{1L} - E_{2L}$ except for overall normalization mentioned above. However the RDWIA calculation reproduces neither the cross section nor the analyzing power. In Fig. 4 the small differences between our calculation and the data in the cross section at larger values of $|E_{1L} - E_{2L}|$ are revealed as the large differences in the analyzing power as in Fig. 2. The RDWIA cannot reproduce the cross section at all. It is also noted that our NR-DWTA calculations in Figs. 1-4 improve old NR-DWTA results [7,16] considerably.

In the NR-DWTA calculations, if the cross section is well reproduced, the analyzing power is also reproduced. Inversely, even small discrepancies with the data of cross section lead to large discrepancies in the analyzing power. This consistency between the calculated cross section and analyzing power is not found in the RDWIA calculations. We consider that absence of the consistency is an essential defect of the RDWIA.

Reference [6] also calculates the analyzing powers at $T_{LAB} = 300$ MeV for outgoing proton angle $(30^\circ, 55^\circ)$. However there are no data of the cross sections, which are necessary for systematic analyses as shown above. Although we do not show figures, our calculations cannot reproduce the data. This is not discouraging because the NR-DWTA does not work well at the asymmetric kinematics of $\theta_{1L} \neq \theta_{2L}$ and $E_{1L} - E_{2L} > 0$ as already seen in Figs. 1 and 2. To the contrary the behavior of RDWIA is inconsistent. It reproduces the analyzing powers for such kinematics at $T_{LAB} = 200$ MeV, but cannot so at $T_{LAB} = 300$ MeV.

As a result of the factorization prescription of Eq. (4), the energy sharing distributions of the cross sections in the NR-DWTA calculation are mainly determined by the distorted momentum distribution of Eq. (10). The success of the NR-DWTA but the failure of the RDWIA to reproduce the cross sections suggests that the factorization is reasonable. In the relativistic approach, the intermediate state $|\mathbf{p}\rangle\langle\mathbf{p}|$ in Eq. (2) is replaced by $|\mathbf{p}+\rangle\langle\mathbf{p}+| + |\mathbf{p}-\rangle\langle\mathbf{p}-|$, where + and - indicate the positive and negative energy states. The contribution of $|\mathbf{p}-\rangle\langle\mathbf{p}-|$ is just the virtual $N\bar{N}$ pair effect. As also pointed out in Ref. [6], it cannot be determined without ambiguity. In this respect we have to note Refs. [17] and [18]. The modified relativistic mean field (RMF) models, in which the effect of negative-energy propagation or the Z-graph contribution is reduced, could reproduce the quasielastic electron scattering [17] and p+A optical potential [18] much better than the original RMF models. Moreover, the ambiguity is not intrinsic to the negative energy state, but intrinsic to the intermediate state itself regardless of positive or negative energy. This is because that the phenomenological NN t -matrix has a physical meaning only for asymptotic positive energy state. Now, the traditional view, which

regards the factorization as a crude approximation [19-21] of the full finite-range DWIA, has to be revised. We want to advocate that the factorization is not an approximation but a reasonable prescription to extract physically meaningful NN t -matrix element relevant to the $(p, 2p)$ reaction from all the matrix elements in the intermediate states.

5 Conclusion

We have reconsidered the NR-DWTA description of the $(p, 2p)$ reaction using modern high-quality phenomenological optical potential and NN t -matrix. The factorized NN t -matrix is directly evaluated in terms of the Dirac spinor and the invariant Fermi amplitude unlike old NR-DWTA calculations. We have calculated $^{40}\text{Ca}(p, 2p)$ reactions at $T_{LAB} = 200$ MeV and compared the results with the RDWIA calculations. It is found that the NR-DWTA results are better than the RDWIA ones especially for the energy sharing distributions of cross sections. More importantly, the NR-DWTA has the consistency between the calculated cross sections and analyzing powers in reproducing experimental data. However it is absent in the RDWIA calculations. Here we present a question. Is the relativistic model really useful to nuclear reactions? Our answer is two-fold. The relativistic description of the phenomenological optical potentials and the NN t -matrix are really useful. These energy-dependent global fittings became possible only after the development of the Dirac approach. To the contrary, the immediate relativistic extension of the NR-DWIA cannot be justified. This is because that the RDWIA assumes unphysical extrapolation of the NN t -matrix to the intermediate state given by elastic distortions. However, for a definitive conclusion, further improvements of both the relativistic and nonrelativistic models are necessary.

Appendix: expressions of $W^{\mu\nu}$

Here we present explicit representations of $W^{\mu\nu}$ s in Eqs. (17) and (18). First, $W_{V_0}^{\mu\nu}$ in Eq. (17) is given by changing the signs of X_i^1 and X_j^2 in $W_S^{\mu\nu}$ of Eqs. (19)-(22),

$$W_{V_0}^{\mu\nu} = W_S^{\mu\nu} (X_i^1 \rightarrow -X_i^1, X_j^2 \rightarrow -X_j^2), \quad (\text{A1})$$

while $W_{V_3}^{\mu\nu}$ are

$$W_{V_3}^{00} = N [X_2^1 (X_1^t - X_2^2) + (X_1^0 + X_1^1) (X_1^2 + X_2^t)], \quad (\text{A2})$$

$$W_{V_3}^{y0} = N [(X_1^1 - X_1^0) (X_1^t - X_2^2) - X_2^1 (X_1^2 + X_2^t)], \quad (\text{A3})$$

$$W_{V_3}^{0y} = N [X_2^1 (X_1^2 - X_2^t) + (X_1^0 + X_1^1) (X_1^t + X_2^2)], \quad (\text{A4})$$

$$W_{V_3}^{yy} = N [(X_1^0 - X_1^1) (X_1^2 - X_2^t) + X_2^1 (X_1^t + X_2^2)], \quad (\text{A5})$$

$$W_{V3}^{xx} = N (X_1^0 - X_1^1) (X_1^2 - X_2^t), \quad (\text{A6})$$

$$W_{V3}^{zz} = N X_2^1 (X_1^t + X_2^2), \quad (\text{A7})$$

$$W_{V3}^{xz} = N (X_1^0 - X_1^1) (X_1^t + X_2^2), \quad (\text{A8})$$

$$W_{V3}^{zx} = N X_2^1 (X_1^2 - X_2^t). \quad (\text{A9})$$

$W_{T0}^{\mu\nu}$ is given by changing the signs of X_i^1 and X_j^2 in $W_{V3}^{\mu\nu}$ of Eqs. (A2)-(A9),

$$W_{T0}^{\mu\nu} = W_{V3}^{\mu\nu} (X_i^1 \rightarrow -X_i^1, X_j^2 \rightarrow -X_j^2), \quad (\text{A10})$$

while $W_{T3}^{\mu\nu}$ are

$$W_{T3}^{00} = N X_1^0 X_2^1 (X_1^2 X_1^t + X_2^2 X_2^t), \quad (\text{A11})$$

$$W_{T3}^{y0} = N (1 + X_1^0 X_1^1) (X_1^2 X_1^t + X_2^2 X_2^t), \quad (\text{A12})$$

$$W_{T3}^{0y} = -N X_1^0 X_2^1 (1 + X_1^2 X_2^t - X_1^t X_2^2), \quad (\text{A13})$$

$$W_{T3}^{yy} = N (1 + X_1^0 X_1^1) (1 + X_1^2 X_2^t - X_1^t X_2^2), \quad (\text{A14})$$

$$W_{T3}^{xx} = N [(1 + X_1^0 X_1^1) (1 + X_1^2 X_2^t + X_1^t X_2^2) + X_1^0 X_2^1 (X_1^2 X_1^t - X_2^2 X_2^t)], \quad (\text{A15})$$

$$W_{T3}^{zz} = N [(1 - X_1^0 X_1^1) (1 - X_1^2 X_2^t - X_1^t X_2^2) + X_1^0 X_2^1 (X_1^2 X_1^t - X_2^2 X_2^t)], \quad (\text{A16})$$

$$W_{T3}^{xz} = N [(1 + X_1^0 X_1^1) (X_2^2 X_2^t - X_1^2 X_1^t) - X_1^0 X_2^1 (1 - X_1^2 X_2^t - X_1^t X_2^2)], \quad (\text{A17})$$

$$W_{T3}^{zx} = N [(1 - X_1^0 X_1^1) (X_2^2 X_2^t - X_1^2 X_1^t) - X_1^0 X_2^1 (1 + X_1^2 X_2^t + X_1^t X_2^2)]. \quad (\text{A18})$$

$W_P^{\mu\nu}$ in Eq. (18) are

$$W_P^{xx} = -N X_2^1 (X_1^t + X_2^2), \quad (\text{A19})$$

$$W_P^{zz} = N (X_1^0 - X_1^1) (X_2^t - X_1^2), \quad (\text{A20})$$

$$W_P^{xz} = N X_2^1 (X_1^2 - X_2^t), \quad (\text{A21})$$

$$W_P^{zx} = N (X_1^0 - X_1^1) (X_1^t + X_2^2). \quad (\text{A22})$$

$W_{A0}^{\mu\nu}$ is given by changing the signs of X_i^1 and X_j^2 in $W_P^{\mu\nu}$ of Eqs. (A19)-(A22),

$$W_{A0}^{\mu\nu} = W_P^{\mu\nu} (X_i^1 \rightarrow -X_i^1, X_j^2 \rightarrow -X_j^2), \quad (\text{A23})$$

while $W_{A3}^{\mu\nu}$ is given by changing the signs of X_i^1 and X_j^2 in $W_{T3}^{\mu\nu}$ of Eqs. (A11)-(A18),

$$W_{A3}^{\mu\nu} = W_{T3}^{\mu\nu} (X_i^1 \rightarrow -X_i^1, X_j^2 \rightarrow -X_j^2). \quad (\text{A24})$$

References

- [1] J.A. McNeil, J.R. Shepard and S.J. Wallace, Phys. Rev. Lett. **50**, 1439 (1983); J.R. Shepard, J.A. McNeil and S.J. Wallace, Phys. Rev. Lett. **50**, 1443 (1983).
- [2] B.C. Clark, S. Hama, R.L. Mercer, L. Ray and B.D. Serot, Phys. Rev. Lett. **50**, 1644 (1983).
- [3] S. Hama, B.C. Clark, E.D. Cooper, H.S. Sherif, R.L. Mercer, Phys. Rev. **C41**, 2737 (1990).
- [4] E.D. Cooper, S. Hama, B.C. Clark and R.L. Mercer, Phys. Rev. **C47**, 297 (1993).
- [5] O.V. Maxwell, Nucl. Phys. **A600**, 509 (1996); **A638**, 747 (1998).
- [6] O.V. Maxwell and E.D. Cooper, Nucl. Phys. **A603**, 441 (1996).
- [7] Y. Kudo and K. Miyazaki, Phys. Rev. **C34**, 1192 (1986).
- [8] G. Jacob and Th.A.J. Maris, Rev. Mod. Phys. **38**, 121 (1966); **45**, 6 (1973).
- [9] T. Berggren and H. Tyrén, Annu. Rev. Nucl. Sci. **16**, 153 (1966).
- [10] D.F. Jackson, in *Advances in Nuclear Physics*, edited by M. Baranger and E. Vogt (Plenum, New York, 1971), Vol.4, p.1.
- [11] R. Bengtsson, T. Berggren, Ch. Gustafsson, Phys. Rep. **41**, 191 (1978).
- [12] P. Kitching, W.J. McDonald, Th.A.J. Maris and C.A.Z. Vasconcellos, in *Advances in Nuclear Physics*, edited by J.W. Negele and E. Vogt (Plenum, New York, 1985), Vol.15, p.43.
- [13] I.E. McCarthy, Introduction to Nuclear Theory, Ch.14 (John Wiley, New York, 1968).
- [14] D.F. Jackson, Nuclear Reactions (Methuen and Co LTD, London, 1970).
- [15] N.S. Chant and P.G. Roos, Phys. Rev. **C27**, 1060 (1983).
- [16] L. Antonuk, *et al.* Nucl. Phys. **A370**, 389 (1982).
- [17] K. Miyazaki, CERN Document Server (CDS) ext-2002-049 revised by Mathematical Physics Preprint Archive (mp_arc) 05-150.
- [18] K. Miyazaki, CERN Document Server (CDS) ext-2002-068 revised by Mathematical Physics Preprint Archive (mp_arc) 05-161.
- [19] N. Austern, Phys. Rev. Lett. **41**, 1696 (1978).

- [20] D.F. Jackson, *Physica Scripta*, **25**, 514 (1982).
- [21] C. Samanta, N.S. Chant, P.G. Roos, A. Nadasen, J. Wesick and A.A. Cowley, *Phys. Rev.* **C34**, 1610 (1986).

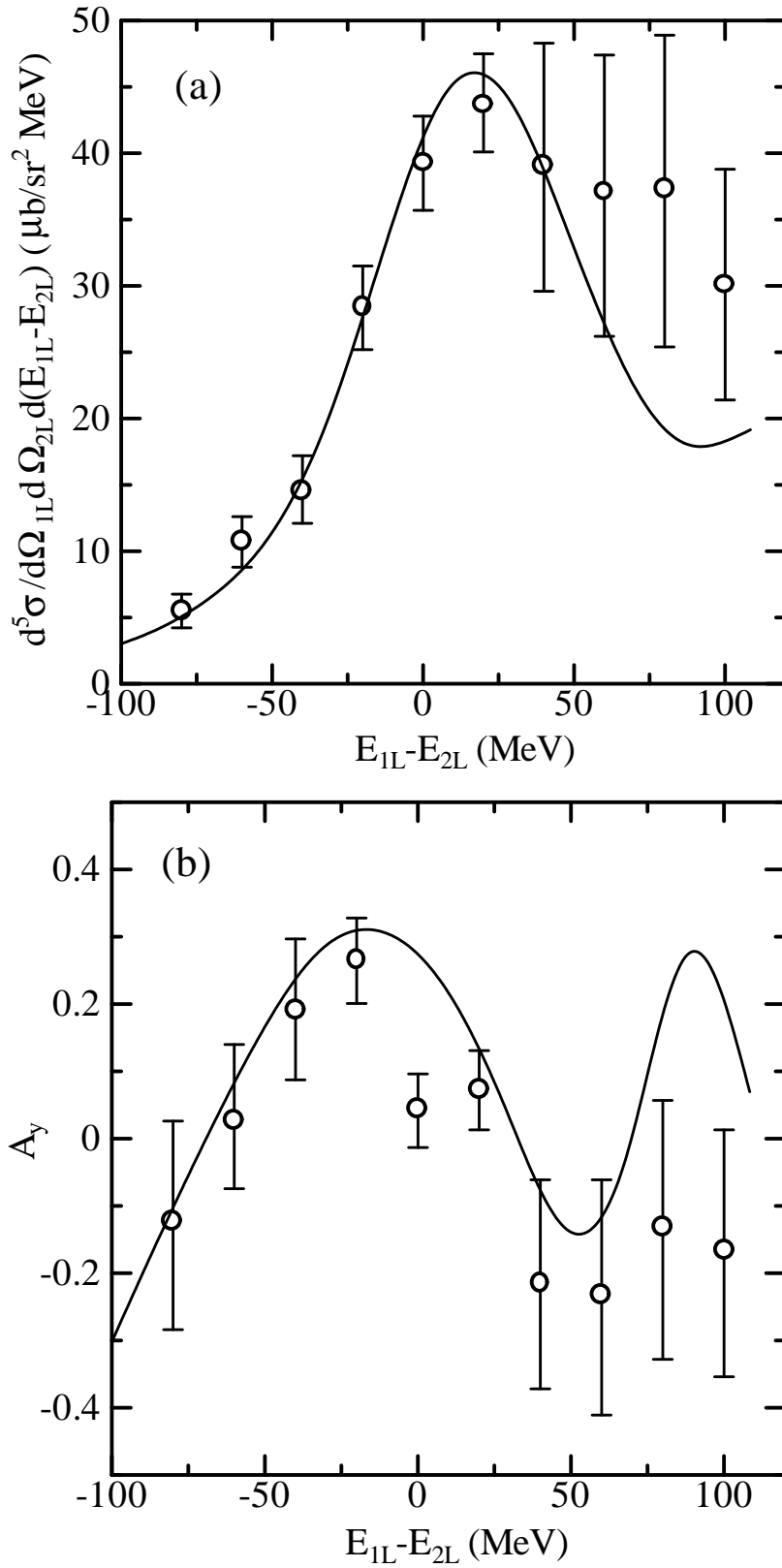


Figure 1: Cross section (a) and analyzing power (b) for proton knockout from the $1d_{3/2}$ state of ^{40}Ca at 200 MeV for outgoing proton angles ($29^\circ, 47^\circ$). The solid curves are the results of NR-DWTA calculation. Experimental data are from Ref. [16].

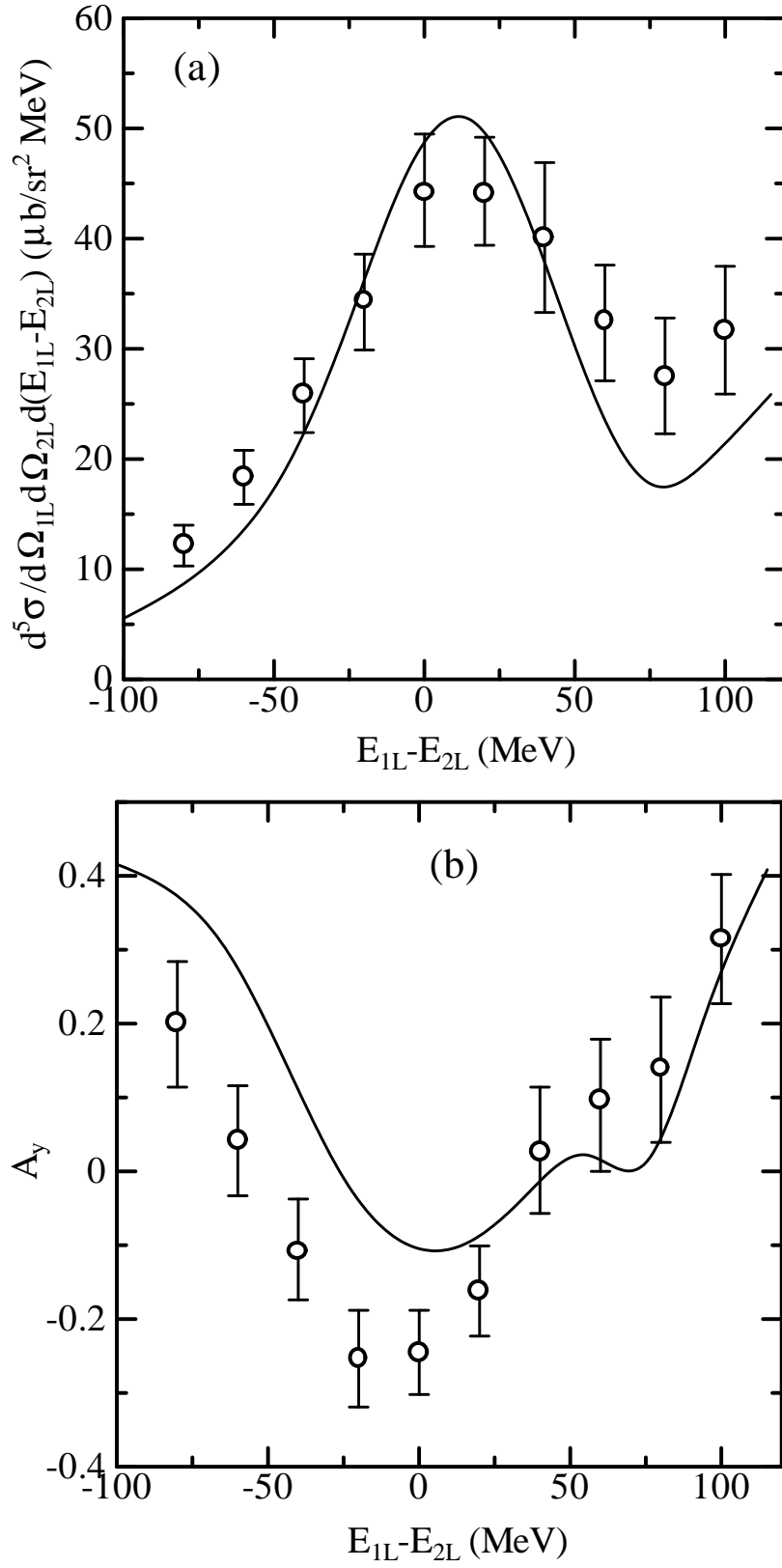


Figure 2: Same as Fig. 1 for proton knockout from the $1d_{5/2}$ state.

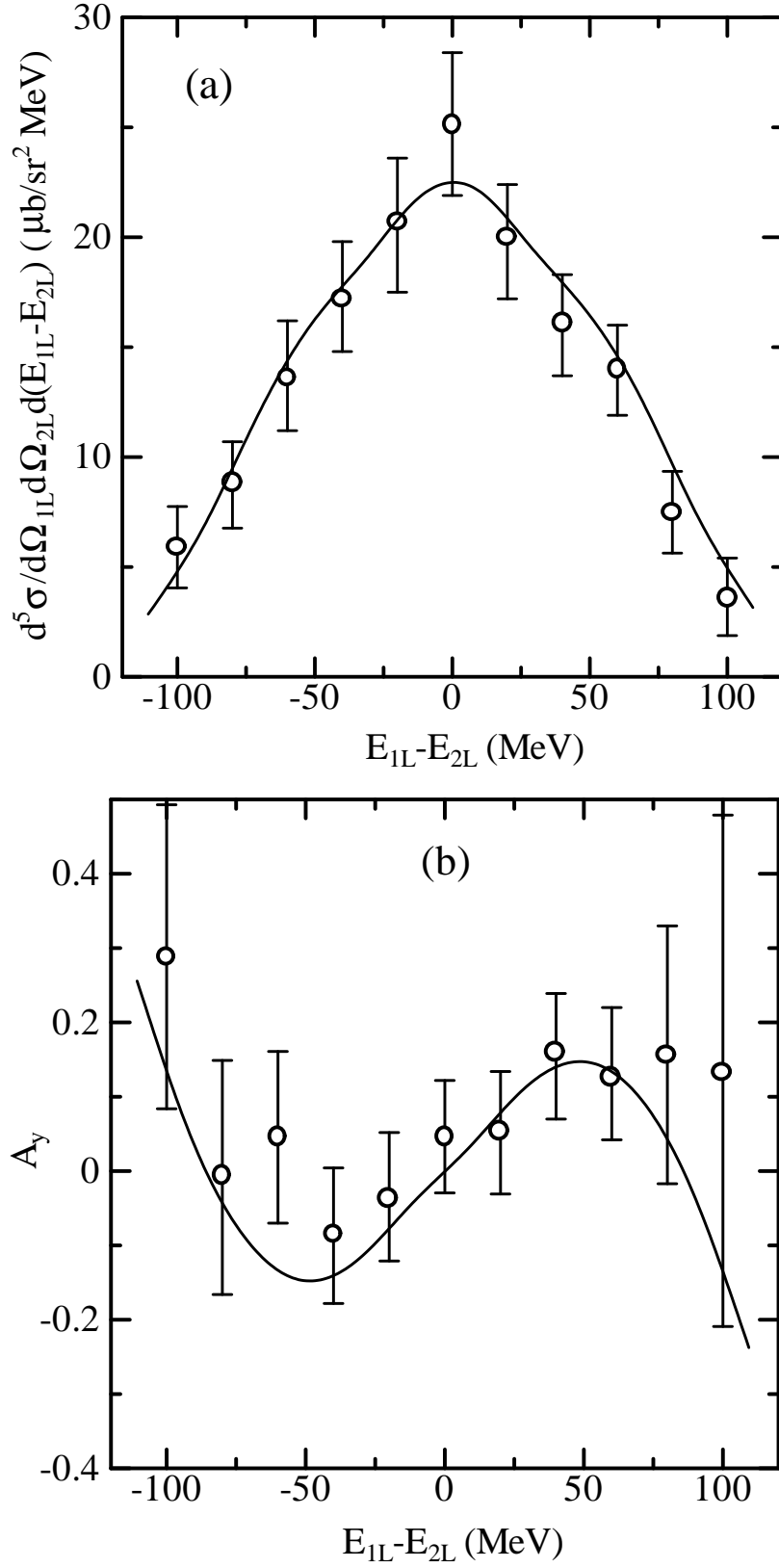


Figure 3: Same as Fig. 1 for outgoing proton angles $(54^\circ, 54^\circ)$.

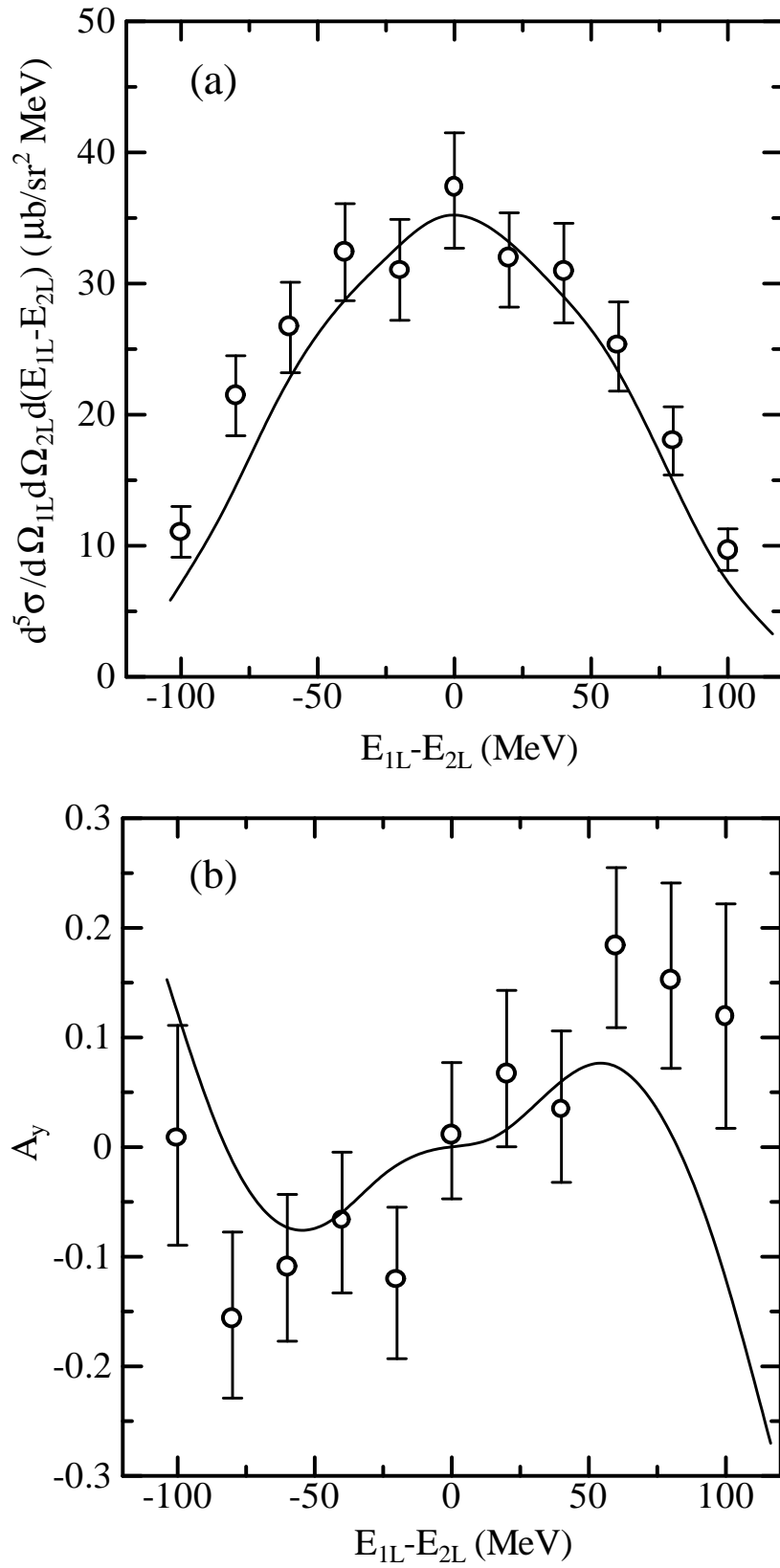


Figure 4: Same as Fig. 3 for proton knockout from the $1d_{5/2}$ state.